



저작자표시-비영리-변경금지 2.0 대한민국

이용자는 아래의 조건을 따르는 경우에 한하여 자유롭게

- 이 저작물을 복제, 배포, 전송, 전시, 공연 및 방송할 수 있습니다.

다음과 같은 조건을 따라야 합니다:



저작자표시. 귀하는 원저작자를 표시하여야 합니다.



비영리. 귀하는 이 저작물을 영리 목적으로 이용할 수 없습니다.



변경금지. 귀하는 이 저작물을 개작, 변형 또는 가공할 수 없습니다.

- 귀하는, 이 저작물의 재이용이나 배포의 경우, 이 저작물에 적용된 이용허락조건을 명확하게 나타내어야 합니다.
- 저작권자로부터 별도의 허가를 받으면 이러한 조건들은 적용되지 않습니다.

저작권법에 따른 이용자의 권리는 위의 내용에 의하여 영향을 받지 않습니다.

이것은 [이용허락규약\(Legal Code\)](#)을 이해하기 쉽게 요약한 것입니다.

[Disclaimer](#)

이학석사학위논문

Altered resting state brain metabolic  
connectivity in dementia with Lewy bodies

루이소체 치매 환자에서 휴지기 뇌 대사 연결성의 변화

2019년 2월

서울대학교 대학원

뇌인지과학과 뇌인지과학전공

최 은 아

# Abstract

## Altered resting state brain metabolic connectivity in dementia with Lewy bodies

Euna Choi

Departement of Brain and Cognitive Science

The Graduate school

Seoul National University

**Objective:** Although Dementia with Lewy bodies (DLB) have Parkinsonism in common with Parkinson's disease (PD) or PD dementia (PDD), they have different neuropathology that underlie Parkinsonism. Altered brain functional connectivity that may correspond to neuropathology has been reported in PD while never been studied in DLB. We compared the resting state metabolic connectivity in striato-thalamo-cortical

(STC) circuit, nigrostriatal pathway, and cerebello-thalamo-cortical motor (CTC) circuit in 27 drug-naïve DLB patients and 27 age- and sex-matched normal controls using <sup>18</sup>F-fluoro-2-deoxyglucose positron emission tomography.

**Methods:** We derived 118 regions of interest (ROIs) using the Automated Anatomical Labeling templates and the Wake Forest University Pick Atlas Tailorach Daemon. We applied the sparse inverse covariance estimation method to construct the metabolic connectivity matrix.

**Results:** DLB patients, with or without Parkinsonism, showed lower inter-regional connectivity between the areas included in the STC circuit (motor cortex – striatum, midbrain – striatum, striatum – globus pallidus, and globus pallidus – thalamus) than the controls. DLB patients with Parkinsonism showed less reduced inter-regional connectivity between midbrain and striatum than those without Parkinsonism, and higher inter-regional connectivity between the areas included in the CTC circuit (motor cortex – pons, pons – cerebellum, and cerebellum – thalamus) than those without Parkinsonism and the controls.

**Interpretation:** Resting state metabolic connectivity in the STC circuit may be reduced in DLB. In DLB with Parkinsonism, CTC circuit and nigrostriatal pathway may be activated to mitigate Parkinsonism. This difference in the brain connectivity may be a candidate biomarker for differentiating DLB from PD or PDD.

**Key words :** Dementia with Lewy bodies, Parkinsonism, Motor circuit, Resting state brain metabolic connectivity

*Student Number* : 2016-20444

## Contents

Page

Abstract .....	i
1. Introduction .....	1
2. Methods .....	3
3. Results .....	8
4. Discussion .....	10
References .....	13
List of Tables .....	19
List of Figures .....	21
국문 초록 .....	28

## 1. Introduction

Dementia with Lewy bodies (DLB) and Parkinson's disease dementia (PDD) together represent the second most common cause of dementia <sup>1</sup>. About 30% of Parkinson's disease (PD) patients have cognitive symptoms at initial diagnosis and as many as 80% will develop cognitive symptoms at some point in their disease <sup>2,3</sup>. About 25-50% of DLB patients show Parkinsonism at initial diagnosis and as many as 80% eventually develop Parkinsonism as the disease progresses <sup>4</sup>. Since PDD commonly show core diagnostic features of DLB, it can be diagnosed when Parkinsonian motor symptoms start at least 1 year earlier than cognitive or perceptual symptoms. In DLB, cognitive symptoms appear before, or at the same time, as motor symptoms <sup>5</sup>. However this 1-year rule has logical and/or practical limitations. For example, it is impossible to distinguish PD from DLB on the 1-year rule when they are prodromal. It is also difficult to determine whether PD with mild cognitive impairment (MCI) would be PDD or DLB <sup>6</sup>.

Although PDD and DLB have Parkinsonism in common, DLB shows more rigidity and bradykinesia than resting tremors, and shows the symptoms more symmetrically than does PDD<sup>7,8</sup>. Although both diseases have Lewy pathology in common, it takes place from brainstem in PD <sup>9,10</sup> while from neocortex or limbic system in DLB <sup>11</sup>. Therefore, we may differentiate PD or PDD from DLB on this different motor pathology even when non-motor symptoms such as cognitive impairment or hallucination are not accompanied.

In PD, nigrostriatal dopaminergic degeneration may produce rigidity and

bradykinesia by impairing the striato-thalamo-cortical (STC) motor circuit.<sup>12</sup> In previous resting state functional magnetic resonance imaging (fMRI) studies, PD showed reduced connectivity between substantia nigra and putamen<sup>13</sup> while enhanced connectivity between motor cortex and striatum<sup>14, 15</sup> and between motor cortex and cerebellum<sup>16</sup>. Since the severity of Parkinsonism was positively correlated with the connectivity of the cerebello-thalamo-cortical (CTC) motor circuit<sup>16</sup>, cerebellum and possibly motor cortex may play a compensatory role to maintain better motor function in PD<sup>17</sup>.

Since DLB has more Lewy pathology in striatum and neocortex<sup>11, 18</sup>, DLB may have different functional connectivity in STC from PD. However, functional connectivity in STC circuit has never been investigated in DLB. In this study, we investigated the connectivity of STC and CTC circuits and nigrostriatal pathway in DLB, by comparing the resting state metabolic connectivity between DLB patients and their age- and sex-matched cognitively normal controls (NC) using <sup>18</sup>F-fluoro-2-deoxyglucose positron emission tomography (FDG-PET).



## **2.Methods**

### **Subjects**

We enrolled 27 DLB patients from visitors to the dementia clinic of Seoul National University Bundang Hospital (SNUBH) from 2006 to 2017, and their 27 age- and sex-matched cognitively NC from visitors to the dementia clinic of SNUBH from 2006 to 2017 and the participants of the Korean Longitudinal Study on Cognitive Aging and Dementia (KLOSCAD). The KLOSCAD is an ongoing nationwide population-based prospective cohort study on cognitive aging and dementia of elderly Koreans launched in 2009 <sup>19</sup>. All subjects were community-dwelling Koreans aged 60 years or older. All DLB patients were naïve from antiparkinsonian or antipsychotic medications and had no other comorbid major psychiatric or neurologic diseases. We summarized the characteristics of the study participants in Table 1.

Geriatric psychiatrists, with expertise in dementia research, administered a standard diagnostic face to face interview, including recording detailed medical histories and conducting physical and neurological examination of each participant, using the Korean version of the Consortium to Establish a Registry for Alzheimer’s Disease Assessment Packet (CERAD-K) Clinical Assessment Battery (CERAD-K-C) <sup>20</sup> and the Korean version of Mini International Neuropsychiatric Interview (MINI) <sup>21</sup>. They evaluated Parkinsonian symptoms using the Extraparamidal Dysfunction in AD (EPDAD) scale included in the CERAD <sup>22</sup>. A research neuropsychologist or trained research nurse conducted neuropsychological assessments, including the CERAD-K-N

<sup>20</sup>, digit span <sup>23</sup>, and frontal assessment battery(FAB) <sup>24</sup>. We also conducted laboratory tests, including complete blood cell counts, chemical profiles, serologic tests for syphilis and typing of apolipoprotein E genes. We diagnosed DLB with the revised consensus criteria proposed by McKeith et al. <sup>11</sup>. Among the 27 DLB patients, 10 either had rigidity or bradykinesia, but no tremor (P+DLB group), but 17 did not have any of the above symptoms (P-DLB group).

### **Image acquisition and preprocessing**

We acquired brain FDG-PET images at the diagnosis from a dedicated PET scanner (Allegro; Philips Medical System, Cleveland, OH, USA) <sup>25</sup> in 54 participants (27 DLB and 27 NC). The amount of intravenous administration of <sup>18</sup>F-FDG was 4.8 MBq/kg for the PET scanner. We instructed the participants to fast for at least 6 hours before scanning. After the fasting period, we checked that the blood sugar level of the participants was below 180 mg/dL. We then injected <sup>18</sup>F-FDG intravenously in a quiet, dimly lit waiting room, and allowed the participants to lie comfortably for a 40 min FDG equilibration period. After the equilibrium period, we led the participants to the adjacent imaging suite and aligned their head to the canthomeatal line in the scanner. From the Allegro PET scanner, we obtained 10-min emission scans and attenuation maps, using a Cs-137 transmission source. We reconstructed attenuation-corrected images using PET data and a 3D row-action maximum-likelihood algorithm with a 3D image filter of 128×128×90 matrices and a pixel size of 2×2×2 mm.

We preprocessed the image data using the Statistical Parametric Mapping 8

(SPM8) software ([www.fil.ion.ucl.ac.uk/spm/](http://www.fil.ion.ucl.ac.uk/spm/)) based on MATLAB 2014a ([www.mathworks.com](http://www.mathworks.com)). We aligned the FDG-PET images of each subject to standard Montreal Neurological Institute (MNI) space by spatial normalization and resampled them to a 2-mm isovoxel resolution <sup>26</sup>. We smoothed all the spatially-normalized PET images using a Gaussian kernel of 8-mm full-width at half maximum (FWHM) to increase the signal-to-noise ratio and to minimize the individual differences in the uncorrected brain cortex. We derived 116 regions of interest (ROIs) consisting of 90 cortical and subcortical regions and 26 cerebellar regions, using the Automated Anatomical Labeling (AAL) templates <sup>27</sup> and 2 ROIs consisting of the brainstem, using the Wake Forest University PickAtlas Tailarach Daemon <sup>28,29</sup>. We calculated regional standard uptake value ratio (SUVR) of each ROI by normalizing to activity in mean values of bilateral postcentral gyrus as a reference region because the postcentral area is a relatively preserved area in DLB <sup>30</sup>.

We defined the 116 ROIs identified above as the nodes and made up the network, with the frontal, motor cortex, parietal, occipital, temporal, insular, thalamus, basal ganglia, brainstem, and cerebellum as 10 subdivisions (Figure 1). We excluded the bilateral postcentral gyrus, used as the reference region. To analyze the connectivity of the STC and CTC circuits, we estimated the resting state metabolic connectivity between seven subdivisions: including motor cortex, striatum, globus pallidus, midbrain, thalamus, pons, and cerebellum. We constructed a subject-by-node matrix (number of subjects  $\times$  116 regions) from each diagnostic group using the SUVR. We applied the sparse inverse covariance estimation (SICE) method to the subject-by-node matrices <sup>31</sup>

using the GraphVar toolbox <sup>32</sup> to construct the metabolic connectivity matrix, in which 0 and 1 represent absence and presence of connections (significant partial correlation between two nodes) at a specific density, respectively. Since SICE does not provide information on strength of metabolic connectivity, we obtained a quasi-measure of the strength by summing the unweighted binary matrices estimated at several different density levels (0.03, 0.05, 0.07, 0.09, 0.12) <sup>31</sup> for visualization purposes (Figure 1L). We visualized the metabolic connectivity matrix on a 3D brain template using the BrainNet toolbox <sup>33</sup> (Figure 1R).

### **Statistical analysis**

We compared the characteristics between diagnostic groups using Chi-squared tests for categorical variables, and independent t-tests or analysis of variance (ANOVA) for continuous variables.

To compare brain connectivity in each group, we calculated the number of connections at a specific threshold (0.03) <sup>31</sup>. The number of connections referred to the number of nodes marked 1 in the metabolic connection matrix. We defined the number of connections between the different subdivisions as inter-regional connectivity, and the number of connections in each subdivision as intra-regional connectivity. For statistical analysis, we extracted 1000 bootstrap samples from each subject group, with replacement. For each of the bootstrap samples, we calculated the number of connections in intra- and inter-subdivisions, as described above <sup>31</sup>. We compared inter-regional connectivities (motor cortex – striatum, midbrain – striatum, striatum – globus pallidus, globus pallidus – thalamus, thalamus – motor cortex, motor cortex – pons, pons –

cerebellum, and cerebellum - thalamus) between P+DLB, P-DLB, and NC groups using ANOVA with Bonferroni post-hoc comparisons. We also compared intra-regional connectivities (motor cortex, midbrain, striatum, globus pallidus, thalamus, pons, and cerebellum) between P+DLB, P-DLB, and NC groups using ANOVA with Bonferroni post-hoc comparisons. We performed all statistical analysis using the IBM SPSS version 20.<sup>34</sup>

### 3. Results

Intra- and inter-regional connectivity matrices of the P+DLB, P-DLB and NC groups are shown in Figure 1. Inter-regional connectivity in the STC and CTC circuits was different between the NC, P+DLB and P-DLB groups; motor cortex – striatum connectivity ( $F_{2,2997} = 1021.02$ ,  $p < 0.001$ ), midbrain – striatum connectivity ( $F_{2,2997} = 153.91$ ,  $p < 0.001$ ), striatum – globus pallidus connectivity ( $F_{2,2997} = 7210.17$ ,  $p < 0.001$ ), globus pallidus – thalamus connectivity ( $F_{2,2997} = 989.52$ ,  $p < 0.001$ ), thalamus – motor cortex connectivity ( $F_{2,2997} = 314.80$ ,  $p < 0.001$ ), motor cortex – pons connectivity ( $F_{2,2997} = 7.04$ ,  $p < 0.001$ ), pons – cerebellum connectivity ( $F_{2,2997} = 148.81$ ,  $p < 0.001$ ), and cerebellum - thalamus connectivity ( $F_{2,2997} = 1248.15$ ,  $p < 0.001$ ). Post-hoc comparisons showed that the inter-regional connectivities within the STC circuit were lower in both P+DLB and P-DLB than in NC. Motor cortex – striatum and striatum – globus pallidus connectivities of P+DLB were comparable to those of P-DLB (Figure 2a and 2e) while globus pallidus – thalamus and midbrain – striatum connectivities of P+DLB were higher than those of P-DLB (Figure 2d and 2f). The inter-regional connectivities within the CTC circuit (motor cortex – pons, pons – cerebellum and cerebellum - thalamus connectivities) of P+DLB were higher than those of P-DLB, as well as those of NC. P-DLB showed comparable connectivity between the motor cortex, pons, cerebellum, and thalamus to NC (Figure 2c, 2g, and 2h). The thalamus – motor cortex connectivity, which is shared by the STC and CTC circuits, was highest in P+DLB, followed by NC and P-DLB (Figure 2b).

As shown in Figure 3, intra-regional connectivity was different between

P+DLB, P-DLB and NC groups in the motor cortex ( $F_{2,2997} = 199.18$ ,  $p < 0.001$ ), striatum ( $F_{2,2997} = 3125.38$ ,  $p < 0.001$ ), globus pallidus ( $F_{2,2997} = 103.65$ ,  $p < 0.001$ ), thalamus ( $F_{2,2997} = 736.23$ ,  $df = 2$ ,  $p < 0.001$ ) and cerebellum ( $F_{2,2997} = 371.608$ ,  $p < 0.001$ ). In these subdivisions, both P+DLB and P-DLB groups showed lower intra-regional connectivity than the NC group. P+DLB group showed comparable intra-regional connectivity to P-DLB in the motor cortex, striatum and globus pallidus (Figure 3a-c) but higher intra-regional connectivity in the thalamus (Figure 3d) and lower intra-regional connectivity in the cerebellum than P-DLB (Figure 3e). Intra-regional connectivity in pons and midbrain were comparable between the three groups.

#### 4. Discussion

In this study, DLB patients, with or without Parkinsonism, showed lower resting metabolic connectivity between the subdivisions included in the STC circuit than the normal controls. Compared to the NC group, both P+DLB and P-DLB groups showed lower inter-regional connectivity between motor cortex – striatum, midbrain – striatum, striatum – globus pallidus, and globus pallidus - thalamus (Figure 2a and 2d-f), and lower intra-regional connectivity in motor cortex, striatum and globus pallidus (Figure 3a-c), indicating that the STC circuit may be disrupted in DLB, regardless of the presence of Parkinsonism. Additionally, P+DLB group showed higher connectivity between midbrain – striatum than the P-DLB group (Figure 2d) and higher motor cortex – pons, pons – cerebellum and cerebellum – thalamus inter-regional connectivity than P-DLB and NC groups (Figure 2c, 2g and 2h), which may be compensatory hyperactivation to mitigate Parkinsonism.

These patterns of resting state brain connectivity of STC circuit and nigrostriatal pathway in DLB contrasted from those reported previously in PD. In previous resting state fMRI studies, PD showed reduced connectivity between substantia nigra and putamen<sup>13</sup> while enhanced inter-regional connectivity between motor cortex and striatum<sup>14, 15</sup> and intra-regional connectivity in motor cortex<sup>35</sup>. This suggests that the relatively preserved motor cortex may compensate the dysfunctional nigrostriatal dopaminergic pathway in PD<sup>36, 37</sup>. The different patterns of brain connectivity observed between DLB and PD seem to reflect the different neuropathology between the two



diseases. In DLB, Lewy pathology is prominent in the neocortex, while in the substantia nigra in PD <sup>9, 11, 38</sup>. Considering that striatal D2 receptor upregulation was observed in PD <sup>39</sup> but not in DLB <sup>18</sup>, the activation of the nigrostriatal dopaminergic projection may play a role in mitigating Parkinsonism in DLB.

This study also found that connectivity in the CTC circuit was enhanced in the P+DLB group as was in PD <sup>16, 40-42</sup>. In PD, compensatory CTC circuit activation was found both at rest and during motor tasks <sup>17</sup>, was positively correlated with the severity of Parkinsonism<sup>16</sup>, and increased with advancing PD <sup>43</sup>. The P+DLB group also showed higher motor cortex – pons, pons – cerebellum and cerebellum – thalamus inter-regional connectivity than the P-DLB and NC groups (Figure 2c, 2g and 2h). In DLB, the CTC circuit may be activated only when Parkinsonism develops to mitigate hypokinetic symptoms as in akinesia/rigidity type PD <sup>16, 40-42</sup>. A recent study confirmed the presence of a disynaptic anatomical connection between the basal ganglia and cerebellum in both animals <sup>44</sup> and humans <sup>45</sup>. Abnormal neural activity in the subthalamic nucleus can be transmitted to the cerebellum via pons <sup>44</sup>. According to the "super-integrator theory", basal ganglia and cerebellar motor thalamus territories assimilate motivational and proprioceptive motor information previously integrated into the cortico-basal ganglia and cortico-cerebellar networks, respectively, to develop sophisticated motor signals that are transmitted in parallel pathways to cortical areas for optimal generation of motor programs <sup>46</sup>. If this is the case, hyperactivation of the cortico-cerebellar network may mitigate Parkinsonism in DLB or PD by affecting the overall CTC circuit through integration in motor thalamus. This may be why the P+DLB group showed higher GP-

TH connectivity than the P-DLB group in the current study (Figure 2f).

This is the first study to investigate the resting state brain metabolic connectivity of DLB using FDG-PET. Resting metabolic connectivity reflects the energy consumption at the metabolic level and reflects synaptic brain metabolism<sup>47</sup>, while the BOLD signal from the functional MRI reflects ongoing neural synchronization<sup>47,48</sup>. Therefore, metabolic connectivity obtained from FDG-PET may better reflect the synaptic dysfunction of neurodegenerative diseases rather than functional connectivity obtained from fMRI<sup>49</sup>. In addition, FDG-PET has better signal-to-noise ratio than fMRI<sup>49</sup>. However, this study has several limitations to be noted. First, the spatial resolution of FDG-PET was not sufficient to separate brain regions into nuclear levels<sup>50</sup>. For example, it is difficult to separate the globus pallidus into an internal part and an external part using FDG-PET. Second, this study was cross-sectional, and the sample size was small. Third, the correlation between the severity of Parkinsonism and the metabolic connectivities in the STC and CTC circuits and nigrostriatal pathway were not investigated.

In DLB patients, resting state metabolic connectivity in the STC circuit was reduced regardless of the presence of Parkinsonism. In DLB patients with Parkinsonism, resting state metabolic connectivity was less reduced in the nigrostriatal pathway than those without Parkinsonism. DLB with Parkinsonism may possibly be differentiated from PD or PDD using the resting state metabolic connectivities of STC and nigrostriatal pathway even when non-motor symptoms appear in DLB.

## References

1. Vann Jones SA, O'Brien JT. The prevalence and incidence of dementia with Lewy bodies: a systematic review of population and clinical studies. *Psychol Med.* 2014 Mar;44(4):673-83.
2. Aldridge GM, Birnschein A, Denburg NL, Narayanan NS. Parkinson's Disease Dementia and Dementia with Lewy Bodies Have Similar Neuropsychological Profiles. *Front Neurol.* 2018;9:123.
3. Emre M, Aarsland D, Brown R, et al. Clinical diagnostic criteria for dementia associated with Parkinson's disease. *Mov Disord.* 2007 Sep 15;22(12):1689-707; quiz 837.
4. McKeith IG, Burn D. Spectrum of Parkinson's disease, Parkinson's dementia, and Lewy body dementia. *Neurol Clin.* 2000;18(4):865-83.
5. McKeith IG, Boeve BF, Dickson DW, et al. Diagnosis and management of dementia with Lewy bodies: Fourth consensus report of the DLB Consortium. *Neurology.* 2017 Jul 4;89(1):88-100.
6. Postuma RB, Berg D, Stern M, et al. Abolishing the 1-year rule: How much evidence will be enough? *Mov Disord.* 2016 Nov;31(11):1623-7.
7. Gnanalingham KK, Byrne EJ, Thornton A, Sambrook MA, Bannister P. Motor and cognitive function in Lewy body dementia: comparison with Alzheimer's and Parkinson's diseases. *J Neurol Neurosurg Psychiatry.* 1997 Mar;62(3):243-52.
8. Aarsland D, Ballard C, McKeith I, Perry RH, Larsen JP. Comparison of extrapyramidal signs in dementia with Lewy bodies and Parkinson's disease. *J Neuropsychiatry Clin Neurosci.* 2001;13(3):374-9.

9. Braak H, Del Tredici K, Rub U, de Vos RA, Jansen Steur EN, Braak E. Staging of brain pathology related to sporadic Parkinson's disease. *Neurobiol Aging*. 2003 Mar-Apr;24(2):197-211.
10. Halliday G, Hely M, Reid W, Morris J. The progression of pathology in longitudinally followed patients with Parkinson's disease. *Acta Neuropathol*. 2008;115(4):409-15.
11. McKeith IG, Dickson DW, Lowe J, et al. Diagnosis and management of dementia with Lewy bodies: third report of the DLB Consortium. *Neurology*. 2005 Dec 27;65(12):1863-72.
12. Bergman H, Wichmann T, Karmon B, DeLong MR. The primate subthalamic nucleus. II. Neuronal activity in the MPTP model of parkinsonism. *J Neurophysiol*. 1994 Aug;72(2):507-20.
13. Wu T, Wang J, Wang C, et al. Basal ganglia circuits changes in Parkinson's disease patients. *Neurosci Lett*. 2012;524(1):55-9.
14. Yu R, Liu B, Wang L, Chen J, Liu X. Enhanced functional connectivity between putamen and supplementary motor area in Parkinson's disease patients. *PLoS One*. 2013;8(3):e59717-e.
15. Kwak Y, Peltier S, Bohnen NI, Muller ML, Dayalu P, Seidler RD. Altered resting state cortico-striatal connectivity in mild to moderate stage Parkinson's disease. *Front Syst Neurosci*. 2010;4:143.
16. Wu T, Wang L, Hallett M, Li K, Chan P. Neural correlates of bimanual anti-phase and in-phase movements in Parkinson's disease. *Brain*. 2010;133(8):2394-409.

17. Wu T, Hallett M. The cerebellum in Parkinson's disease. *Brain*. 2013 Mar;136(Pt 3):696-709.
18. Piggott M, Marshall E, Thomas N, et al. Striatal dopaminergic markers in dementia with Lewy bodies, Alzheimer's and Parkinson's diseases: rostrocaudal distribution. *Brain*. 1999;122(8):1449-68.
19. Han JW, Kim TH, Kwak KP, et al. Overview of the Korean Longitudinal Study on Cognitive Aging and Dementia. *Psychiatry Investig*. 2018 Aug;15(8):767-74.
20. Lee JH, Lee KU, Lee DY, et al. Development of the Korean Version of the Consortium to Establish a Registry for Alzheimer's Disease Assessment Packet (CERAD-K) Clinical and Neuropsychological Assessment Batteries. *The Journals of Gerontology: Series B*. 2002;57(1):P47-P53.
21. Yoo S-W, Kim Y-S, Noh J-S, et al. Validity of Korean version of the mini-international neuropsychiatric interview. *Anxiety Mood*. 2006;2.
22. Fillenbaum GG, van Belle G, Morris JC, et al. Consortium to Establish a Registry for Alzheimer's Disease (CERAD): the first twenty years. *Alzheimers Dement*. 2008 Mar;4(2):96-109.
23. Wechsler memory scale—revised WD. Manual.—New York: The psychological corporation harcourt Brace Jovanovicch. Inc, 1987—150 p. 1987.
24. Dubois B, Slachevsky A, Litvan I, Pillon B. The FAB: a frontal assessment battery at bedside. *Neurology*. 2000;55(11):1621-6.
25. Kang JY, Lee WW, So Y, Lee BC, Kim SE. Clinical Usefulness of (18)F-fluoride Bone PET. *Nucl Med Mol Imaging*. 2010 Apr;44(1):55-61.

26. Della Rosa PA, Cerami C, Gallivanone F, et al. A standardized [18F]-FDG-PET template for spatial normalization in statistical parametric mapping of dementia. *Neuroinformatics*. 2014 Oct;12(4):575-93.
27. Tzourio-Mazoyer N, Landeau B, Papathanassiou D, et al. Automated anatomical labeling of activations in SPM using a macroscopic anatomical parcellation of the MNI MRI single-subject brain. *Neuroimage*. 2002 Jan;15(1):273-89.
28. Lancaster JL, Woldorff MG, Parsons LM, et al. Automated Talairach atlas labels for functional brain mapping. *Hum Brain Mapp*. 2000;10(3):120-31.
29. Maldjian JA, Laurienti PJ, Kraft RA, Burdette JH. An automated method for neuroanatomic and cytoarchitectonic atlas-based interrogation of fMRI data sets. *Neuroimage*. 2003 Jul;19(3):1233-9.
30. Albin R, Minoshima S, D'amato C, Frey K, Kuhl D, Sima A. Fluoro-deoxyglucose positron emission tomography in diffuse Lewy body disease. *Neurology*. 1996;47(2):462-6.
31. Huang S, Li J, Sun L, et al. Learning brain connectivity of Alzheimer's disease by sparse inverse covariance estimation. *Neuroimage*. 2010 Apr 15;50(3):935-49.
32. Kruschwitz JD, List D, Waller L, Rubinov M, Walter H. GraphVar: a user-friendly toolbox for comprehensive graph analyses of functional brain connectivity. *J Neurosci Methods*. 2015 Apr 30;245:107-15.
33. Xia M, Wang J, He Y. BrainNet Viewer: A Network Visualization Tool for Human Brain Connectomics. *PLoS One*. 2013;8(7):e68910.
34. SPSS I. IBM SPSS statistics for Windows, version 20.0. New York: IBM Corp.

2011.

35. Wu T, Long X, Wang L, et al. Functional connectivity of cortical motor areas in the resting state in Parkinson's disease. *Hum Brain Mapp.* 2011 Sep;32(9):1443-57.

36. Grafton ST. Contributions of functional imaging to understanding parkinsonian symptoms. *Curr Opin Neurobiol.* 2004 Dec;14(6):715-9.

37. Peraza LR, Nesbitt D, Lawson RA, et al. Intra- and inter-network functional alterations in Parkinson's disease with mild cognitive impairment. *Hum Brain Mapp.* 2017 Mar;38(3):1702-15.

38. Cersosimo MG. Propagation of alpha-synuclein pathology from the olfactory bulb: possible role in the pathogenesis of dementia with Lewy bodies. *Cell Tissue Res.* 2017:1-11.

39. Kaasinen V, Ruottinen HM, Nagren K, Lehtikainen P, Oikonen V, Rinne JO. Upregulation of putaminal dopamine D2 receptors in early Parkinson's disease: a comparative PET study with [11C] raclopride and [11C]N-methylspiperone. *J Nucl Med.* 2000 Jan;41(1):65-70.

40. Wu T, Hallett M. A functional MRI study of automatic movements in patients with Parkinson's disease. *Brain.* 2005;128(10):2250-9.

41. Wu T, Wang L, Hallett M, Chen Y, Li K, Chan P. Effective connectivity of brain networks during self-initiated movement in Parkinson's disease. *Neuroimage.* 2011;55(1):204-15.

42. Cerasa A, Hagberg GE, Peppe A, et al. Functional changes in the activity of cerebellum and frontostriatal regions during externally and internally timed movement in

Parkinson's disease. *Brain Res Bull.* 2006 Dec 11;71(1-3):259-69.

43. Sen S, Kawaguchi A, Truong Y, Lewis MM, Huang X. Dynamic changes in cerebello-thalamo-cortical motor circuitry during progression of Parkinson's disease. *Neuroscience.* 2010 Mar 17;166(2):712-9.

44. Bostan AC, Dum RP, Strick PL. The basal ganglia communicate with the cerebellum. *Proc Natl Acad Sci U S A.* 2010;107(18):8452-6.

45. Milardi D, Arrigo A, Anastasi G, et al. Extensive Direct Subcortical Cerebellum-Basal Ganglia Connections in Human Brain as Revealed by Constrained Spherical Deconvolution Tractography. *Front Neuroanat.* 2016;10:29-.

46. Bosch-Bouju C, Hyland BI, Parr-Brownlie LC. Motor thalamus integration of cortical, cerebellar and basal ganglia information: implications for normal and parkinsonian conditions. *Front Comput Neurosci.* 2013;7:163.

47. Viswanathan A, Freeman RD. Neurometabolic coupling in cerebral cortex reflects synaptic more than spiking activity. *Nat Neurosci.* 2007 Oct;10(10):1308-12.

48. Di X, Biswal BB, Alzheimer's Disease Neuroimaging I. Metabolic brain covariant networks as revealed by FDG-PET with reference to resting-state fMRI networks. *Brain Connect.* 2012;2(5):275-83.

49. Yakushev I, Drzezga A, Habeck C. Metabolic connectivity: methods and applications. *Curr Opin Neurol.* 2017 Dec;30(6):677-85.

50. Moses WW. Fundamental Limits of Spatial Resolution in PET. *Nucl Instrum Methods Phys Res A.* 2011;648 Supplement 1:S236-S40.



## List of Tables

Table 1. Characteristics of the participants

Table 1. Characteristics of the participants

	NC (N = 27)	DLB			<i>p</i>	
		All (N = 27)	P-DLB (N = 17)	P+DLB (N = 10)	NC vs All DLB	NC vs P-DLB vs P+DLB
Age (years, mean $\pm$ SD)	73.3 $\pm$ 5.3	72.7 $\pm$ 5.2	71.6 $\pm$ 4.5	74.7 $\pm$ 5.9	1.000	0.579
Sex (Women, %)	63.0	63.0	70.6	50.00	0.680	0.564
Education (years, mean $\pm$ SD)	12.6 $\pm$ 4.4	11.2 $\pm$ 5.4	11.1 $\pm$ 4.8	11.5 $\pm$ 6.6	0.298	0.571
MMSE (points, mean $\pm$ SD)	26.3 $\pm$ 2.3	21.1 $\pm$ 5.1	22.5 $\pm$ 4.8	18.6 $\pm$ 4.7	< 0.001	< 0.001

MMSE = Mini-Mental State Examination, SD = Standard deviation. Chi-squared tests for categorical variables and independent t-test or analysis of variance for continuous variables. ANOVA test was performed for three group comparisons.

## List of Figures

Figure 1. Intra- and inter-regional connectivity matrices of the P+DLB, P-DLB and NC groups.

Figure 2. Comparison of the number of inter-regional connections among P+DLB, P-DLB and NC groups.

Figure 3. Comparison of the number of intra-regional connections among P+DLB, P-DLB, and NC groups.

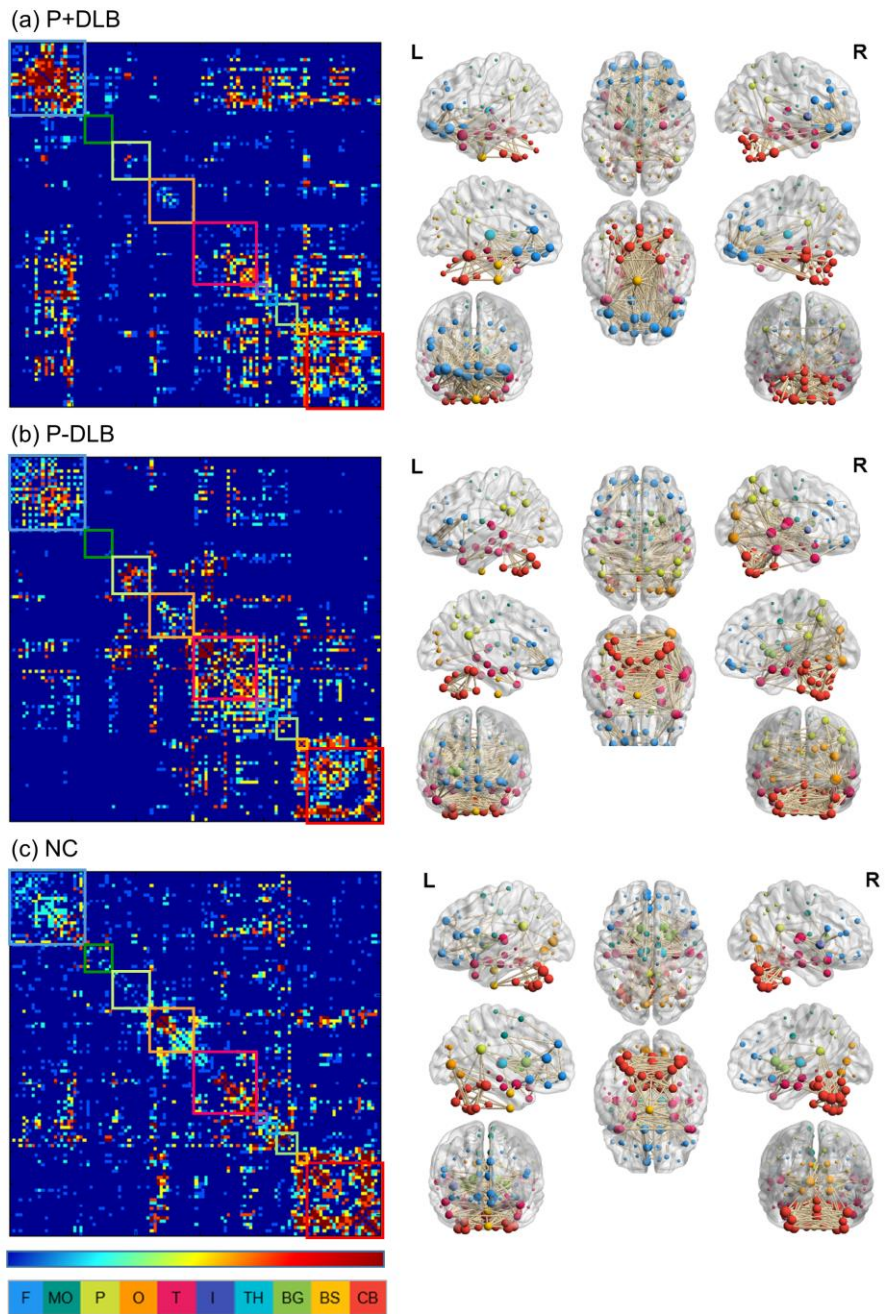


**Figure 1.** Intra- and inter-regional connectivity matrices of the P+DLB, P-DLB and NC

groups. Full connectivity matrices in the left column were obtained from 116 nodes. The color bar represents the strength of connectivity, with red representing stronger connectivity, and blue representing weaker connectivity. Each box represents the 10 subdivisions, which are: F, MC, P, O, T, I, TH, BF, BS and CB (see abbreviations below). The color of each subdivision matches the color of the node in the brain template in the right column. We display connectivity matrices on 3D brain templates on the right column.

Abbreviations: P+DLB, dementia with Lewy bodies with parkinsonism; P-DLB, dementia with Lewy bodies without parkinsonism; NC, normal controls; F, frontal; MC, motor cortex; P, parietal; O, occipital; T, temporal; I, insular; TH, thalamus; BG, basal ganglia; BS, brainstem; CB, cerebellum

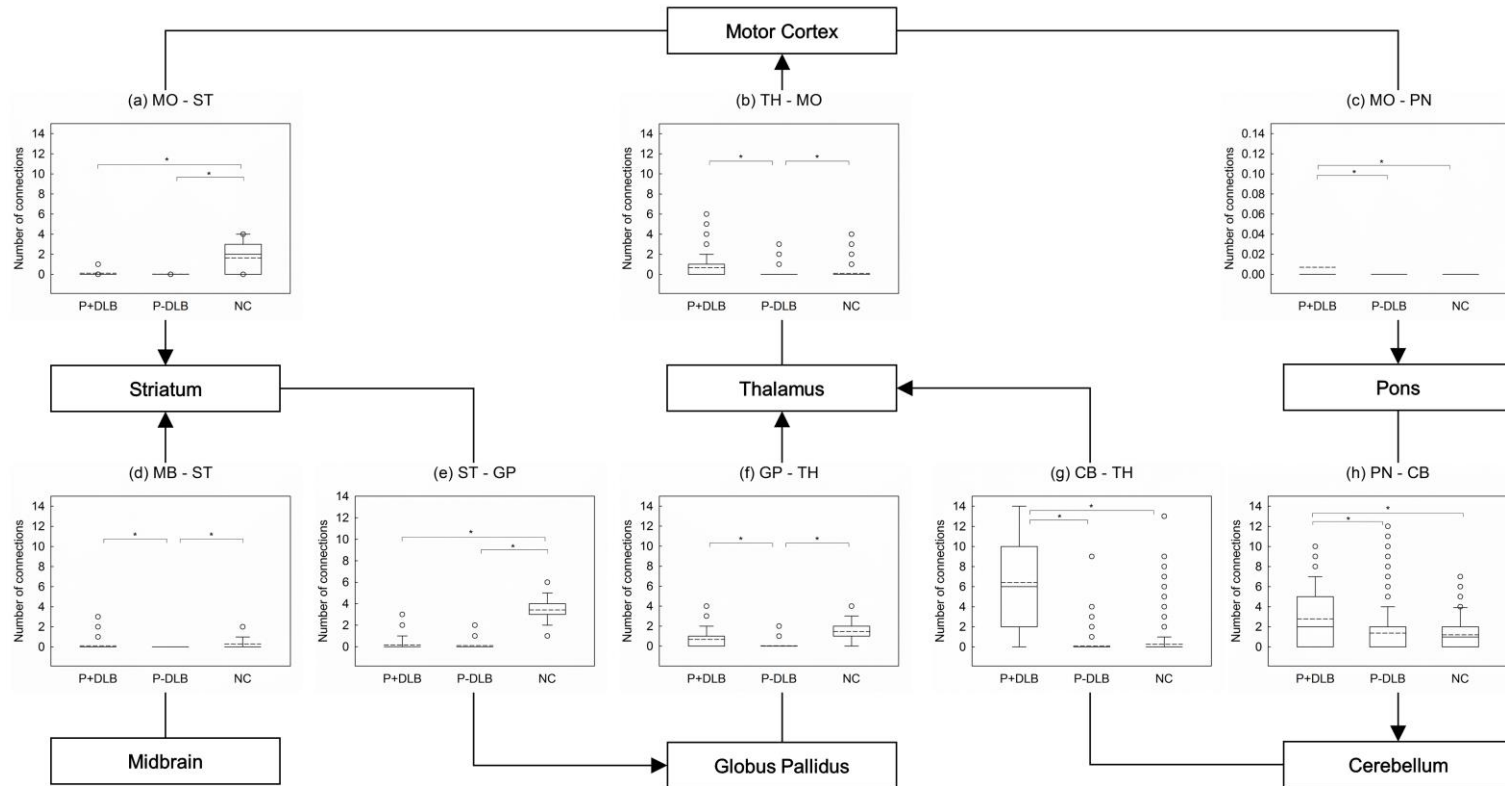


Figure 2. Comparison of the number of inter-regional connections among P+DLB, P-DLB and NC groups. Box plots of the mean

number of connections between (a) MC–ST; (b) MC-PN, (c) TH-MC, (d) MB-ST, (e) ST-GP, (f) GP-TH, (g) CB-TH and (h) PN-CB.

Solid lines represent the median value and dashed lines represent the mean value.

Abbreviations: P+DLB, dementia with Lewy bodies with parkinsonism; P-DLB, dementia with Lewy bodies without parkinsonism;

NC, normal controls; MC, motor cortex; ST, striatum; PN, pons; TH, thalamus; MB, midbrain; GP, globus pallidus; CB, cerebellum

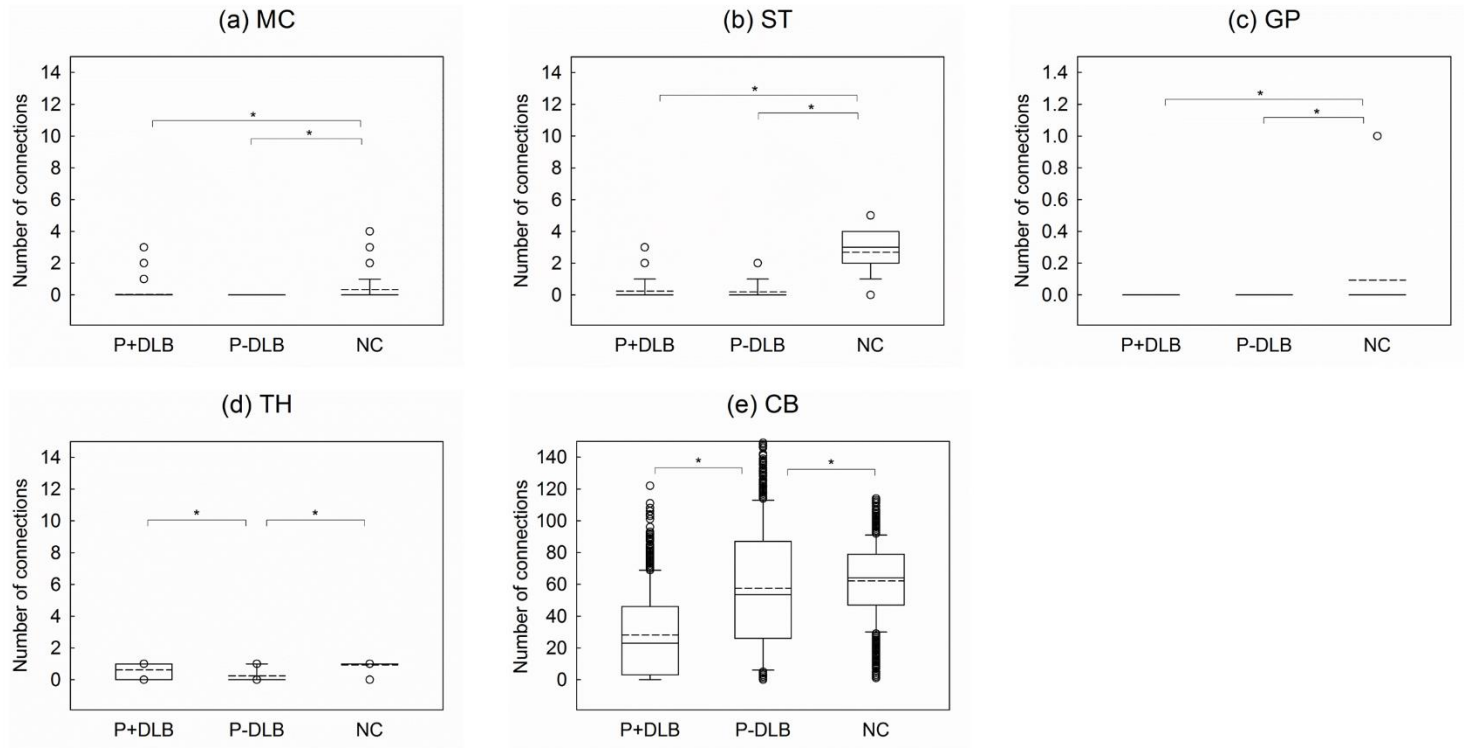


Figure 3. Comparison of the number of intra-regional connections among P+DLB, P-DLB, and NC groups. Box plots of the mean number of connections between: (a) MC, (b) ST, (c) GP, (d) TH and (e) CB. Solid lines represent the median value and dashed lines



represent the mean value.

Abbreviations: P+DLB, dementia with Lewy bodies with parkinsonism; P-DLB, dementia with Lewy bodies without parkinsonism;

NC, normal controls; MC, motor cortex; ST, striatum; GP, globus pallidus; TH, thalamus; CB, cerebellum

# 국문 초록

**배경** : 루이소체 치매 (DLB)는 파킨슨병 (PD)이나 파킨슨 치매 (PDD)와 공통으로 파킨슨 증상을 가지지만, 이들은 파킨슨 증상의 기초가 되는 신경 병리학은 다르다. 파킨슨 증상의 신경 병리학에 해당하는 뇌의 기능적 연결성 변화는 파킨슨병에서는 보고되었지만, 루이소체 치매에서는 알려진 바 없다. 우리는 약물을 복용 이력이 없는 루이소체 환자 27명과 나이와 성별을 고려한 정상 대조군 27명을 대상으로 양전자 방출 단층 촬영 (18F-FDG-PET) 을 이용하여 선조체-시상-피질 운동회로 와 흑질-선조체 경로, 소뇌-시상-피질 회로의 휴지기 뇌 대사 연결성을 비교했다.

**방법** : Automated Anatomical Labeling templates와 the Wake Forest University Pick Atlas Tailarach Daemon을 사용하여 118개의 관심 영역 (ROI) 을 추출했다. 우리는 sparse inverse covariance estimation (SICE) 방법을 적용하여 대사 연결 행렬을 구성했다.

**결과** : 파킨슨증상 유무에 관계없이 DLB 환자는 정상군보다 선조체-시상-피질 운동회로 (운동피질 - 선조체, 중뇌 - 선조체, 선조체 - 담창구, 담창구 - 시상) 에서 낮은 지역간 연결성이 나타났다. 파킨슨 증상이 있는 DLB 환자들은 파킨슨 증상이 없는 DLB환자들보다 중뇌-선조체 사이의 지역간 연결성이 낮았고, 소뇌-시상-피질 운동회로 (운동피질 - 교뇌, 교뇌-소뇌, 소뇌-시상)의 연결성이 높았다.

**해석**: DLB에서 선조체-시상-피질 운동회로의 휴지기 뇌 대사 연결성이 감소했다. 파킨슨 증상이 있는 DLB 환자에서 파킨슨 증상을 완화하기 위해 소뇌-시상-피질 운동회로와 흑질-선조체 경로가 활성화 되었을 것이다. 이러한 휴지기 뇌 대사 연결성의 차이는 DLB와 PD 또는 DLB와 PDD를 구별하기 위한 잠재적인 바이오마커의 가능성이 있다.

**주요어** : 루이소체 치매, 파킨슨증상, 운동회로, 휴지기 뇌 대사 연결성

학번: 2016-20444